# Paleohistology of the intercentra of North American metoposaurids from the Upper Triassic of Petrified Forest National Park (Arizona, USA) with implications for the taxonomy and ontogeny of the group (#14552)

First submission

Please read the **Important notes** below, the **Review guidance** on page 2 and our **Standout reviewing tips** on page 3. When ready **submit online**. The manuscript starts on page 4.

#### Important notes

#### **Editor and deadline**

Andrew Farke / 11 Jan 2017

Files 8 Figure file(s)

2 Table file(s)

Please visit the overview page to **download and review** the files

not included in this review PDF.

**Declarations** No notable declarations are present

2



Please read in full before you begin

#### How to review

When ready <u>submit your review online</u>. The review form is divided into 5 sections. Please consider these when composing your review:

- 1. BASIC REPORTING
- 2. EXPERIMENTAL DESIGN
- 3. VALIDITY OF THE FINDINGS
- 4. General comments
- 5. Confidential notes to the editor
- 1 You can also annotate this PDF and upload it as part of your review

To finish, enter your editorial recommendation (accept, revise or reject) and submit.

#### **BASIC REPORTING**

- Clear, unambiguous, professional English language used throughout.
- Intro & background to show context.
  Literature well referenced & relevant.
- Structure conforms to **PeerJ standards**, discipline norm, or improved for clarity.
- Figures are relevant, high quality, well labelled & described.
- Raw data supplied (see **PeerJ policy**).

#### **EXPERIMENTAL DESIGN**

- Original primary research within **Scope of** the journal.
- Research question well defined, relevant & meaningful. It is stated how the research fills an identified knowledge gap.
- Rigorous investigation performed to a high technical & ethical standard.
- Methods described with sufficient detail & information to replicate.

#### **VALIDITY OF THE FINDINGS**

- Impact and novelty not assessed.
  Negative/inconclusive results accepted.
  Meaningful replication encouraged where rationale & benefit to literature is clearly stated.
- Data is robust, statistically sound, & controlled.
- Conclusions are well stated, linked to original research question & limited to supporting results.
- Speculation is welcome, but should be identified as such.

The above is the editorial criteria summary. To view in full visit <a href="https://peerj.com/about/editorial-criteria/">https://peerj.com/about/editorial-criteria/</a>

# 7 Standout reviewing tips



The best reviewers use these techniques

	n
	N

# Support criticisms with evidence from the text or from other sources

# Give specific suggestions on how to improve the manuscript

# Comment on language and grammar issues

# Organize by importance of the issues, and number your points

# Give specific suggestions on how to improve the manuscript

# Please provide constructive criticism, and avoid personal opinions

# Comment on strengths (as well as weaknesses) of the manuscript

#### **Example**

Smith et al (J of Methodology, 2005, V3, pp 123) have shown that the analysis you use in Lines 241-250 is not the most appropriate for this situation. Please explain why you used this method.

Your introduction needs more detail. I suggest that you improve the description at lines 57-86 to provide more justification for your study (specifically, you should expand upon the knowledge gap being filled).

The English language should be improved to ensure that your international audience can clearly understand your text. I suggest that you have a native English speaking colleague review your manuscript. Some examples where the language could be improved include lines 23, 77, 121, 128 - the current phrasing makes comprehension difficult.

- 1. Your most important issue
- 2. The next most important item
- 3. ...
- 4. The least important points

Line 56: Note that experimental data on sprawling animals needs to be updated. Line 66: Please consider exchanging "modern" with "cursorial".

I thank you for providing the raw data, however your supplemental files need more descriptive metadata identifiers to be useful to future readers. Although your results are compelling, the data analysis should be improved in the following ways: AA, BB, CC

I commend the authors for their extensive data set, compiled over many years of detailed fieldwork. In addition, the manuscript is clearly written in professional, unambiguous language. If there is a weakness, it is in the statistical analysis (as I have noted above) which should be improved upon before Acceptance.



# Paleohistology of the intercentra of North American metoposaurids from the Upper Triassic of Petrified Forest National Park (Arizona, USA) with implications for the taxonomy and ontogeny of the group

Bryan M Gee  $^{\text{Corresp.,}\ 1}$  , William G Parker  $^2$  , Adam D Marsh  $^2$ 

Corresponding Author: Bryan M Gee Email address: bryan.gee@mail.utoronto.ca

Metoposaurids are temnospondyl amphibians that are commonly collected from the Chinle Formation deposits of North America. Two species, *Koskinondon perfectus* and *Apachesaurus gregorii* are known from Petrified Forest National Park, AZ, USA. Small, elongate intercentra are the single diagnostic postcranial characteristic of the smaller *A. gregorii*. However, a poor understanding of the earliest life stages of *K. perfectus* and other large metoposaurids makes it unclear whether the proportions of the intercentra are a diagnostic feature for species discrimination or whether they are influenced by ontogeny. Previous work on metoposaurid intercentra has proven that ontogenetic information can be extrapolated from histological analyses. Here we perform a histological analysis of metoposaurid intercentra from Petrified Forest National Park and our results suggest that the elongate intercentra are the consequence of ontogenetic variation rather than speciation.

 $<sup>^{</sup>m 1}$  Department of Biology, University of Toronto Mississauga, Ontario, Canada

<sup>&</sup>lt;sup>2</sup> Division of Science and Resource Management, Petrified Forest National Park, Arizona, United States of America





1	Paleohistology of the intercentra of North American metoposaurids from the Upper
2	Triassic of Petrified Forest National Park (Arizona, USA) with implications for the
3	taxonomy and ontogeny of the group
4	
5	Bryan M. Gee <sup>1</sup> ; William G. Parker <sup>2</sup> ; Adam D. Marsh <sup>2</sup>
6	<sup>1</sup> Department of Biology, University of Toronto Mississauga, ON, Canada
7	<sup>2</sup> Division of Science and Resource Management, Petrified Forest National Park, AZ, USA
8	
9	Corresponding author:
10	Bryan M. Gee
11	
12	Corresponding email: <u>bryan.gee@mail.utoronto.ca</u>
13	
14	
15	
16	
17	
18	
19	
20	
21	
22	
23	
24	
25	
26	
27	
28	
29	
30	
31	



32 **Abstract.** Metoposaurids are temnospondyl amphibians that are commonly collected from the 33 Chinle Formation deposits of North America. Two species, Koskinondon perfectus and 34 Apachesaurus gregorii are known from Petrified Forest National Park, AZ, USA. Small, 35 elongate intercentra are the single diagnostic postcranial characteristic of the smaller A. gregorii. 36 However, a poor understanding of the earliest life stages of *K. perfectus* and other large 37 metoposaurids makes it unclear whether the proportions of the intercentra are a diagnostic 38 feature for species discrimination or whether they are influenced by ontogeny. Previous work on metoposaurid intercentra has proven that ontogenetic information can be extrapolated from 39 40 histological analyses. Here we perform a histological analysis of metoposaurid intercentra from Petrified Forest National Park and our results suggest that the elongate intercentra are the 41 42 consequence of ontogenetic variation rather than speciation. 43 **Introduction.** Metoposaurids are Late Triassic temnospondyl amphibians with a global 44 45 distribution and are some of the most commonly collected fossils from freshwater depositional settings in the Chinle Formation (Hunt, 1993). There are presently three valid taxa of 46 47 metoposaurids in North America: two of large size, Koskinonodon perfectus and K. bakeri, and 48 one of small size, Apachesaurus gregorii (Case, 1922, 1931; Branson & Mehl, 1929; Hunt, 1993; Mueller, 2007). Two of these, K. perfectus and A. gregorii are known from Petrified Forest 49 50 National Park (PEFO), AZ, USA (Hunt & Lucas, 1993; Long & Murry, 1995; Heckert & Lucas, 51 2002; Parker & Martz, 2011). The former is common in the lower units within the Chinle 52 Formation (Blue Mesa Member and lower part of the Sonsela Member) and is rare in the upper 53 units (the upper part of the Sonsela Member and the Petrified Forest Member) (Hunt & Lucas, 54 1993; Heckert & Lucas, 2002; Parker & Martz, 2011). A. gregorii demonstrates the opposite 55 pattern of stratigraphic distribution (Parker and Martz, 2011). Although fossils of A. gregorii are 56 relatively common, the vast majority of them consist of isolated, elongate intercentra. 57 Additionally, while the diagnosis of A. gregorii includes a wide set of cranial traits, only a 58 shallow otic notch can be confirmed by more than one specimen (Spielmann & Lucas, 2012). 59 Finally, while size has frequently been used as an informal characteristic in identifying 60 specimens (A. gregorii being significantly smaller than all other metoposaurid taxa), this is not a 61 reliable metric given the role of ontogeny in changing body size (Horner, De Ricglès & Padian, 62 1998; Horner & Goodwin, 2009; Werning, 2012). As a result, the diagnosis of A. gregorii based



53	on elongate intercentra is tentative in the absence of multiple specimens that can confirm more of
54	the diagnostic cranial features. Because growth series for North American metoposaurids are not
65	well known, particularly among the earliest life stages, it remains unclear whether the diagnostic
66	anatomy of A. gregorii is the product of speciation or if it are merely a misinterpretation of
67	features influenced by ontogeny. Such a possibility is rarely considered in determining whether
68	small metoposaurid specimens are skeletally mature individuals of A. gregorii or skeletally
59	immature individuals of either Koskinonodon species. In this study, we focus on analyzing the
70	single diagnostic postcranial trait of A. gregorii, elongate intercentra.
71	
72	Bone histology is a common method used to study ontogeny in a variety of extinct taxa, often by
73	comparison to extant members of these clades (Padian, 2013). Although the majority of
74	paleohistological inquiries have centered on amniotes, several workers have previously
75	performed histological analyses on temnospondyls (e.g., Steyer et al., 2004; Witzmann & Soler-
76	Gijon, 2010; Sanchez & Schoch, 2013). Most of these analyses have examined long bones, as is
77	conventional for other tetrapods (e.g. Konietzko-Meier & Sander, 2013). Histology of
78	temnospondyl intercentra has been performed only a handful of times (e.g., Mukherjee, Ray &
79	Sengupta, 2010; Konietzko-Meier, Danto & Gadek, 2014; Danto, Witzmann & Fröbisch, 2016),
30	and the only previous examination of metoposaurid intercentra was conducted on the European
31	taxon Metoposaurus krasiejowensis (Konietzko-Meier, Bodzioch & Sander, 2012).
32	Metoposaurid intercentra spanning a wide size range are commonly recovered elements at
33	PEFO, making them more accessible for histology than the relatively rare limb elements. This
34	study seeks to provide an alternative approach to comparisons of external morphology in order to
35	evaluate the potential for metoposaurid intercentra proportions to be influenced by ontogeny
36	rather than speciation.
37	
88	Keywords: paleohistology, ontogeny, metoposaurid
39	Institutional Abbreviations: NMMNH: New Mexico Museum of Natural History and Science,
90	Albuqerque, NM, USA; PEFO: Petrified Forest National Park, AZ, USA; UOPB, University of
91	Opole, Department of Biosystematics, Opole, Poland.
92	
93	Materials and Methods.



94	Selection of specimens
95	All material referenced here was collected from the Late Triassic sedimentary rocks of the
96	Chinle Formation at Petrified Forest National Park, AZ, USA. Metoposaurids are found
97	throughout three commonly occurring units of the Chinle (the Blue Mesa Member, Sonsela
98	Member, and Petrified Forest Member), but there are disparate relative abundances of large and
99	small metoposaurids throughout the stratigraphic column. Eight of the ten elements were
100	selected with the goal of sampling an intercentrum of shortened proportions normally referred to
101	K. perfectus and an intercentrum of elongate proportions normally referred to A. gregorii from
102	the same stratigraphic horizon, if not the same locality (Table 1, Fig. 3). PEFO 4826 and PEFO
103	38726 are from locality PFV 122 in the Blue Mesa Member (Fig. 1-2). PEFO 38645 is from PFV
104	040 in the Petrified Forest Member (Fig. 1-2). PEFO 36874 and PEFO 16696 (two and three
105	intercentra, respectively) are from a locality (PFV 215) in the Petrified Forest Member (Fig. 1-2)
106	Elements are assigned to the same specimen number on the basis of physical proximity during
107	collection and general taxonomic identity and should not be interpreted to mean that the elements
108	are from the same individual. The final two intercentra, belonging to PEFO 35392 (also from
109	PFV 215), were selected because of their association with a skull of a small metoposaurid that
110	was interpreted to be a juvenile K. perfectus (B.M. Gee & W.G. Parker, unpublished data).
_	
111	Specimens were measured using the same standards as Konietzko-Meier, Bodzioch & Sander
111	Specimens were measured using the same standards as Konietzko-Meier, Bodzioch & Sander
111 112	Specimens were measured using the same standards as Konietzko-Meier, Bodzioch & Sander (2012). The overall size range of the elements sampled in this study (mediolateral width between
<ul><li>111</li><li>112</li><li>113</li></ul>	Specimens were measured using the same standards as Konietzko-Meier, Bodzioch & Sander (2012). The overall size range of the elements sampled in this study (mediolateral width between 9.81 mm and 55.32 mm) is similar to that sampled by the motivational study (mediolateral width
<ul><li>111</li><li>112</li><li>113</li><li>114</li></ul>	Specimens were measured using the same standards as Konietzko-Meier, Bodzioch & Sander (2012). The overall size range of the elements sampled in this study (mediolateral width between 9.81 mm and 55.32 mm) is similar to that sampled by the motivational study (mediolateral width
<ul><li>111</li><li>112</li><li>113</li><li>114</li><li>115</li></ul>	Specimens were measured using the same standards as Konietzko-Meier, Bodzioch & Sander (2012). The overall size range of the elements sampled in this study (mediolateral width between 9.81 mm and 55.32 mm) is similar to that sampled by the motivational study (mediolateral width between 20.1 mm and 71 mm; Konietzko-Meier, Bodzioch & Sander, 2012).
<ul><li>111</li><li>112</li><li>113</li><li>114</li><li>115</li><li>116</li></ul>	Specimens were measured using the same standards as Konietzko-Meier, Bodzioch & Sander (2012). The overall size range of the elements sampled in this study (mediolateral width between 9.81 mm and 55.32 mm) is similar to that sampled by the motivational study (mediolateral width between 20.1 mm and 71 mm; Konietzko-Meier, Bodzioch & Sander, 2012).  **Classification of specimens' axial position**
<ul><li>111</li><li>112</li><li>113</li><li>114</li><li>115</li><li>116</li><li>117</li></ul>	Specimens were measured using the same standards as Konietzko-Meier, Bodzioch & Sander (2012). The overall size range of the elements sampled in this study (mediolateral width between 9.81 mm and 55.32 mm) is similar to that sampled by the motivational study (mediolateral width between 20.1 mm and 71 mm; Konietzko-Meier, Bodzioch & Sander, 2012).  **Classification of specimens' axial position**  Because North American metoposaurids, especially those from PEFO, are rarely articulated,
111 112 113 114 115 116 117 118	Specimens were measured using the same standards as Konietzko-Meier, Bodzioch & Sander (2012). The overall size range of the elements sampled in this study (mediolateral width between 9.81 mm and 55.32 mm) is similar to that sampled by the motivational study (mediolateral width between 20.1 mm and 71 mm; Konietzko-Meier, Bodzioch & Sander, 2012).  **Classification of specimens' axial position**  Because North American metoposaurids, especially those from PEFO, are rarely articulated, determining the exact serial position of the studied vertebrae remains difficult. Vertebrae are
111 112 113 114 115 116 117 118 119	Specimens were measured using the same standards as Konietzko-Meier, Bodzioch & Sander (2012). The overall size range of the elements sampled in this study (mediolateral width between 9.81 mm and 55.32 mm) is similar to that sampled by the motivational study (mediolateral width between 20.1 mm and 71 mm; Konietzko-Meier, Bodzioch & Sander, 2012).  **Classification of specimens' axial position**  Because North American metoposaurids, especially those from PEFO, are rarely articulated, determining the exact serial position of the studied vertebrae remains difficult. Vertebrae are placed using previously-outlined criteria (Sulej, 2007), but it should be noted that these criteria
111 112 113 114 115 116 117 118 119 120	Specimens were measured using the same standards as Konietzko-Meier, Bodzioch & Sander (2012). The overall size range of the elements sampled in this study (mediolateral width between 9.81 mm and 55.32 mm) is similar to that sampled by the motivational study (mediolateral width between 20.1 mm and 71 mm; Konietzko-Meier, Bodzioch & Sander, 2012).  **Classification of specimens' axial position**  Because North American metoposaurids, especially those from PEFO, are rarely articulated, determining the exact serial position of the studied vertebrae remains difficult. Vertebrae are placed using previously-outlined criteria (Sulej, 2007), but it should be noted that these criteria were used in the description of *Metoposaurus krasiejowensis** and it remains unknown what
111 112 113 114 115 116 117 118 119 120 121	Specimens were measured using the same standards as Konietzko-Meier, Bodzioch & Sander (2012). The overall size range of the elements sampled in this study (mediolateral width between 9.81 mm and 55.32 mm) is similar to that sampled by the motivational study (mediolateral width between 20.1 mm and 71 mm; Konietzko-Meier, Bodzioch & Sander, 2012).  **Classification of specimens' axial position**  Because North American metoposaurids, especially those from PEFO, are rarely articulated, determining the exact serial position of the studied vertebrae remains difficult. Vertebrae are placed using previously-outlined criteria (Sulej, 2007), but it should be noted that these criteria were used in the description of *Metoposaurus krasiejowensis** and it remains unknown what differences may exist in the vertebral column between the European and North American taxa,
111 112 113 114 115 116 117 118 119 120 121 122	Specimens were measured using the same standards as Konietzko-Meier, Bodzioch & Sander (2012). The overall size range of the elements sampled in this study (mediolateral width between 9.81 mm and 55.32 mm) is similar to that sampled by the motivational study (mediolateral width between 20.1 mm and 71 mm; Konietzko-Meier, Bodzioch & Sander, 2012).  **Classification of specimens' axial position**  Because North American metoposaurids, especially those from PEFO, are rarely articulated, determining the exact serial position of the studied vertebrae remains difficult. Vertebrae are placed using previously-outlined criteria (Sulej, 2007), but it should be noted that these criteria were used in the description of *Metoposaurus krasiejowensis** and it remains unknown what differences may exist in the vertebral column between the European and North American taxa, especially in the absence of preserved neural or haemal arches. Additionally, intraspecific

125	
126	Thin section preparation and imaging
127	The intercentra were first cleaned using a toothbrush and water to remove excess matrix before
128	being consolidated with Paraloid B-72 (Rohm and Haas) dissolved in acetone. All specimens
129	were molded and casted according to PEFO museum standards, with Carbowax (molecular
130	weight 4000; Dow) added to stabilize cracks and other fragile areas. After creating two-part
131	molds using (I need to send you latex info), the Carbowax was removed using a brush and warm
132	water. All specimens were impregnated in a polyester resin mixture of Castolite <sup>TM</sup> AC and
133	hardener (Eager Polymers) at a ratio of 1 oz of Castolite <sup>TM</sup> to 12 drops of hardener. The
134	specimens were placed in a vacuum chamber to evacuate gas from the resin and then allowed to
135	cure for a minimum of 24 hours. Because the primary focus of the study was to assess the
136	ontogenetic stage of various intercentra to determine whether small, elongate intercentra ascribed
137	to A. gregorii belonged to juveniles of K. perfectus, we decided to focus on sagittal cuts (down
138	the midline in the anteroposterior axis) based on the amount of ontogenetic information that
139	could be derived from the different planes in the analysis of Konietzko-Meier, Bodzioch &
140	Sander (2012). All specimens were cut using an automated IsoMet 1000 Precision Saw
141	(Buehler). The cut surface of the desired block and its respective thin section were prepared by
142	polishing each with a 600-mesh silicon carbide on (include make, model, rpm with parent
143	company in parentheses). Both surfaces were rinsed with ethanol and then attached to plexiglass
144	slides using Scotch-Weld Instant Adhesive (CA40; 3M). The sections were allowed to dry for a
145	minimum of 1 hour. All specimens except PEFO 38726 were cut to a height of 0.7 mm using the
146	IsoMet 1000 Precision Saw. PEFO 38726 was too large to be cut by the automatic saw, so it was
147	cut manually by hand with a larger saw fitting for the IsoMet. All specimens were polished in the
148	following sequence: Hillquist 1010 grinding cup, 600-mesh grit, 1000-mesh grit, 1-micron grit.
149	PEFO 38726 was polished on a 600-mesh lap wheel before polishing on the Hillquist to remove
150	uneven surfaces from the manual cut. The thin sections were gradually ground down with
151	repeated examination under a compound microscope to evaluate their optical clarity. All
152	polishing after the Hillquist step was done manually on glass plates. Thin sections were imaged
153	on a Nikon Instruments AZ100 Multizoom microscope fitted with AZ-Plan Apo 0.5x and AZ-
154	Fluor 5x objective lenses, an AZ-RP rotatable polarizer plate, and a DS-Fi2 digital camera
155	mount. NIS-Elements imaging software was used for this study.
155	mount. NIS-Elements imaging software was used for this study.



156	
157	
158	Results.
159	Microanatomy and general histology
160	Overall, the composition and structure of the intercentra sampled is very similar to those that
161	were described for Metoposaurus krasiejowensis (Konietzko-Meier, Bodzioch & Sander, 2012).
162	At peripheral surfaces that were preserved, endochondral bone is found on the anterior and
163	posterior faces and at the dorsal surface where the intercentrum would have been attached to the
164	neural spine (Fig. 4). The ventral surface is formed by endochondral trabecular bone in younger
165	individuals and by an external cortex in more mature individuals (Fig. 4). With the exception of
166	the smallest intercentra that fall outside of the lower size bound of the sampled specimens of $M$ .
167	krasiejowensis (Konietzko-Meier, Bodzioch & Sander, 2012), a distinct region of periosteal bone
168	is present in a triangular shape, with the apex ventral to the geometrical center of the element in
169	all but some of the largest intercentra (Fig. 4G-H). This triangular region is separated from the
170	endochondral region by obliquely-oriented trabeculae (Fig. 4). Within the periosteal region, the
171	layers are densely packed and oriented parallel to the ventral surface of the intercentrum in
172	contrast to the random arrangement of endochondral bone (Fig. 4). In some of the larger
173	specimens, the periosteal region lacks the densely packed matrix (Fig. 4B, 4H-I). This does not
174	appear to be ontogenetic in nature because PEFO 38726, the largest specimen, features a densely
175	layered periosteal region in the absence of secondary mineral precipitation that characterizes all
176	specimens with open periosteal regions (Fig. 4J). Additionally, some of the smaller specimens,
177	such as PEFO 36874a, feature reduced secondary mineralization that only damages the local
178	areas of the periosteal region in which it occurs (Fig. 4B).
179	
180	For this study, we utilize the formal Histological Ontogenetic Stages (HOS) that were created for
181	M. krasiejowensis by Konietzko-Meier, Bodzioch, & Sander (2012). The nature of the periosteal
182	bone is used to characterize the ontogenetic stage of an individual; HOS 1 lacks any periosteal
183	ossification, HOS 2 features a wide periosteal bone, HOS 3 features decreased vascularization in
184	the external cortex, and HOS 4 features LAGs in the external cortex (Konietzko-Meier,
185	Bodzioch, & Sander 2012). The ontogenetic assignments are summarized below in Table 2.
186	





187	<i>PEFO 16696</i> (Fig. 4B, 4D, 4H, 5C, 6C, 7C, 8C-D): PEFO 16696a is similar to PEFO 4826 in
188	having a fully open notochordal channel filled with secondary minerals (Fig. 5C). The periosteal
189	region is semi-circular as in the smaller intercentra, but the layered matrix is significantly more
190	disperse (Fig. 6C). The presence of secondary mineral precipitates, a feature also seen in the
191	periosteal region of PEFO 35392, PEFO 36874b, PEFO 38645, and PEFO 16696c, appears to be
192	responsible for the absence of densely layered matrix in the region (Fig 6C). Additionally, the
193	endochondral bone in the dorsal half of PEFO 16696a is significantly more disperse than in
194	larger specimens sampled here, although the endochondral bone on the articular faces is thicker
195	and more densely packed, as observed in all other intercentra (Fig. 4B, Fig. 7C). Relative to
196	larger intercentra, the marginal endochondral bone appears to be more vascularized. PEFO
197	16696b and PEFO 16696c share many features with other large intercentra. The periosteal region
198	is triangular in shape and consists of a parallel-layered matrix (Fig. 8D). In PEFO 16696b, the
199	apex that terminates ventral to the mid-height of the element, while in PEFO 16696c, it
200	terminates at or slightly above this point (Fig. 4D, Fig. 4H). In PEFO 16696c, some layers of the
201	periosteal region appear to have been destroyed by precipitation of secondary minerals, a
202	recurring feature in some of the larger intercentra, which makes it difficult to identify the exact
203	point of termination of the apex. The endochondral bone is thickest at the articular surfaces and
204	is more disperse in the internal cavity. There is no evidence of an external cortex in PEFO
205	16696a and PEFO 16696b. In PEFO 16696c, an external cortex is present, but it is well
206	vascularized and shows no evidence of LAGs (Fig. 8C). We assign PEFO 16696a and PEFO
207	16696b to HOS 2. PEFO 16696c is assigned to HOS 3 but is considered to be relatively
208	immature in comparison to other specimens of the same assignment.
209	
210	PEFO 35392 (Fig. 4G, 4I, 8B): Both of these elements are associated with a partial skull that
211	was interpreted as a juvenile K. perfectus by B.M. Gee & W.G. Parker (unpublished data). The
212	histological characterization of these intercentra supports the terpretation, as they feature a
213	relatively wide periosteal region and a moderate degree of vascularization in the external cortex
214	region (Fig. 4G, 4I). Both elements are similar to each other and to other intercentra lacking a
215	notochordal channel that were sampled in this study. The periosteal region is triangular in shape
216	with an apex that terminates well below the mid-height of the intercentrum in PEFO 35392a
217	(Fig. 4G) and an apex that terminates around that point in PEFO 35392b (Fig. 4I). The matrix of





218	parallel layers is much less dense and coincides with the presence of secondary carbonate
219	minerals, which likely damaged the region, making it difficult to discern the exact point at which
220	the apex terminates in PEFO 35392b (Fig. 4I). The endochondral bone is relatively intact and is
221	similar to other intercentra in being densest at the articular faces and randomly distributed
222	throughout the internal cavity. A weathered external cortex is preserved in both of the specimens,
223	but appears to still be relatively well vascularized and shows no evidence of LAGs where present
224	(Fig. 8B). We assign both specimens to HOS 3.
225	
226	PEFO 36874 (Fig. 4A, 4F, 5B, 6B, 7B): The smaller of the two elements assigned to this
227	specimen (PEFO 36874a) differs from PEFO 4826 and PEFO 16696a in having a notochordal
228	channel that appears to be in the early stages of ossification. Tissue deposition originates around
229	the geometric center of the element and probably spread outward throughout ossification based
230	on the characterization of the notochordal pits in larger specimens (Fig. 5B). In this specimen,
231	tissue from the two halves appears to have recently connected prior to the death of the individual.
232	The overall shape of the periosteal region of PEFO 36874a is similar to the semi-circular contour
233	of the other small intercentra (Fig. 6B). PEFO 36874b features a typical morphology of the
234	larger intercentra sampled in this study: a triangular periosteal region with an apex terminating
235	ventral to the mid-height of the element, dense endochondral bone on the articular surfaces, and
236	more disperse, vascularized endochondral bone in the internal cavity (Fig. 4F). As in several
237	other intercentra, the periosteal region lacks a densely layered matrix but co-occurs with a
238	similar concentration of secondary carbonate minerals. An external cortex does not appear to be
239	present in PEFO 36874a, and in PEFO 36874b, it is highly vascularized with no evidence of
240	LAGs (Fig. 4A, 4F). We assign PEFO 3 to HOS 2 and PEFO 36874b to HOS 3.
241	
242	PEFO 38645 (Fig. 4E, 8A): This specimen shows no evidence of a notochordal channel. The
243	periosteal region is comparable to other specimens in having a parallel-layered matrix and an
244	apex that terminates below the mid-height of the intercentrum (Fig. 4E). The periosteal region
245	lacks a densely layered matrix, as in PEFO 35392 and PEFO 36874b, but also features a high
246	degree of secondary carbonate precipitation that likely damaged the internal structure (Fig. 4E).
247	One articular surface was damaged during preparation of the thin section, but the other shows a
248	dense endochondral bone layer with tighter packing than the elements of PEFO 35392. Similar to



249	PEFO 368/4, a posterior protrusion on the dorsal surface that may be a remnant of the neural
250	arch is preserved (Fig. 4E). The remainder of the endochondral bone in the internal cavity is
251	otherwise modestly vascularized and randomly oriented. The external cortex is relatively well
252	preserved and compact, similar to PEFO 38726, but there is no evidence of LAGs or any
253	taphonomic damage that may have erased them (Fig. 8A). We assign this specimen to HOS 3
254	and note that it is more mature than the elements of PEFO 35392.
255	
256	PEFO 38726 (Fig. 4J, 8D): This specimen is the largest analyzed in this study and shows no
257	evidence of a notochordal channel. The periosteal region consists of a dense matrix of parallel
258	layers and is triangular in shape with an apex that terminates at or before the mid-height of the
259	element (Fig. 4J). The external cortex of this specimen is relatively well preserved and shows a
260	reduced degree of vascularization compared to the smaller specimens. At least two light-colored
261	bands can be seen in the cortex and run parallel to the ventral surface of the intercentrum (Fig.
262	8D). They are continuous throughout the well-preserved portion of this area, which leads us to
263	tentatively conclude that these are LAGs. As in other intercentra, the endochondral bone on the
264	articular surfaces is thicker and more densely packed than in the internal cavity. On the dorsal
265	surface, an elevated posterior protrusion may be the remnants of a neural arch that was lost
266	during preservation (Fig. 4J). We assign this specimen to HOS 4.
267	
268	PEFO 4826 (Fig. 4C, 5A, 6A, 7A): This specimen is the largest of the three intercentra that
269	feature an open notochordal channel. The notochordal channel is obstructed only by secondary
270	matrix; its dorsal and ventral walls are nearly flat (Fig. 5A). The periosteal region is semi-
271	circular, as in the PEFO 16696a and PEFO 36874a, with a dense matrix of parallel layers
272	running in the anterior-posterior axis (Fig. 6A). There is no evidence of taphonomic damage that
273	resulted in the absence of a compact external cortex with LAGs. The endochondral bone in the
274	dorsal portion of the intercentrum shows an intermediate degree of vascularization in being more
275	densely packed than the other two small intercentra and less densely packed than in larger
276	intercentra with a closed notochordal channel (Fig. 7A). Dense endochondral bone also forms the
277	margins on the anterior and posterior articular surfaces. The dorsal margin of the element is
278	slightly damaged, which is common in North American metoposaurids owing to the removal of
279	the neural arches during preservation. We assign this specimen to HOS 2.

280

281	<b>Discussion.</b> The most significant finding of this study is the confirmation that, at least in some
282	instances, small intercentra of proportions referable to A. gregorii belong to highly immature
283	individuals. Two prominent features inform the ontogenetic assignment of these specimens: (1) a
284	perforate notochordal channel and (2) a wide, more semi-circular periosteal region (Fig. 5-6).
285	These structures are found in the three smallest intercentra (PEFO 4826, PEFO 16696a, PEFO
286	36874a) and provide insight into the ontogenetic changes in the internal structure of the axial
287	column in metoposaurids. We are confident that the open notochordal channel is a juvenile
288	feature because its closure is widespread in Triassic temnospondyls, including metoposaurids
289	(Warren & Snell, 1991). The notochordal channel closes and is gradually reduced to a pair of
290	perforations, one on each articular surface, that migrate dorsally and eventually disappear in
291	some species (Warren & Snell, 1991; Danto, Witzmann & Fröbisch, 2016). Based on
292	comparisons to described vertebral series in M. krasiejowensis, M. bakeri, Dutuitosaurus
293	ouazzoui and isolated intercentra of K. perfectus, this pattern often terminates in an entirely
294	smooth articular surface with no notochordal perforation in mature individuals (Case, 1932;
295	Dutuit, 1976; Warren & Snell, 1991; Sulej, 2007). Additionally, we can be certain that the
296	notochordal channel does close in smaller individuals with elongate intercentra based on PEFO
297	36874a, which captures the onset of this ossification and is discussed further below (Fig. 5B).
298	The designation of the three smallest intercentra as belonging to juvenile individuals is also
299	supported by the wide periosteal region, which originates near the anteroventral and
300	posteroventral margins, forming a shallow concave depression rather than the distinct triangle
301	seen in larger intercentra of this study and the intercentra of Metoposaurus (Konietzko-Meier,
302	Bodzioch & Sander, 2012). In all three of the smallest PEFO specimens, the apex of the
303	periosteal region terminates well before reaching the dorsal surface of the ventral half (Fig. 6).
304	Finally, the small intercentra show other evidence of a relatively immature ontogenetic stage,
305	such as the absence of thick ventral trabeculae near the external surface, the absence of LAGs,
306	and less densely packed endochondral bone in the dorsal portion of the intercentrum in
307	comparison to larger specimens (Fig. 4A-C, Fig. 5-6). As a result, we can be confident that the
308	ossification of the notochordal channel did not occur relatively late in ontogeny and conclude
309	that all three of the small intercentra belong to an early ontogenetic stage of a large metoposauric
310	rather than to A. gregorii. Larger sampled intercentra also show evidence of relative immaturity





311 up to the largest specimen, PEFO 38726, when LAGs appear in the external cortex (Fig. 8D). 312 Although the material is from a variety of localities and stratigraphic horizons, increased size of 313 the sampled intercentra always produced more ontogenetically mature structures, leading us to 314 conclude that that the sampled material can be compiled into a composite growth series. Because 315 K. bakeri has not been identified west of Texas, and its intercentra differ from that of K. perfectus with regard to the notochordal channel (discussed below), we tentatively assign this 316 317 material to K. perfectus, with the understanding that future revision may be necessary as more diagnostic material is recovered (Hunt, 1993; Long & Murry, 1995). It is possible that the onset 318 319 of ossification of the notochordal channel reflects a milestone in the development of K. perfectus. 320 In light of the hypothesis suggesting that *Koskinonodon* could have had ecologically separated 321 life stages (Rinehart et al., 2009), the ossification of the intercentra could potentially represent 322 the onset of a more aquatic lifestyle. 323 324 This study has also produced an unexpected finding that suggests some differences in the 325 ontogenetic trajectory of K. perfectus in relation to other metoposaurids with known vertebral 326 columns. In the original description of K. bakeri, Case (1932) noted that the presence of a 327 notochordal channel and its persistence as reduced perforations on the articular surfaces in more 328 mature specimens differed from other metoposaurid specimens from Texas, presumably of K. 329 perfectus, in that the known material of the latter lacked any sort of perforation. This pattern also 330 appears in the intercentra of K. perfectus that are described or figured in other publications (e.g., Colbert & Imbrie, 1956; Hunt, 1993; Long & Murry, 1995; Spielmann & Lucas, 2012). We have 331 332 also found this same pattern in an informal survey of several dozen metoposaurid intercentra in the collections at PEFO. This suggests that with regards to timing, the ossification of the 333 334 notochordal canal occurs much earlier in K. perfectus. We also note that the smallest specimen 335 analyzed by Konietzko-Meier, Bodzioch & Sander (2012), an early juvenile (UOPB 00117), is 336 larger than two of the three small intercentra sampled here (PEFO 16696a, PEFO 36874a) but is 337 classified as being more ontogenetically immature (HOS 1) than either due to the absence of 338 periosteal ossification (Fig. 5, Table 2). It may be that K. perfectus juveniles experienced a 339 relatively rapid burst of growth and tissue reorganization within the skeleton in comparison to M. *krasiejowensis*, possibly as a result of environmental triggers, but this hypothesis requires 340 341 additional sampling to test. Finally, only the largest intercentra sampled in our study (PEFO





342	38/26) contains possible LAGs in the external cortex (Fig. 8D). This element is most
343	comparable in size to UOPB 00115, which they classified as a late juvenile (Konietzko-Meier,
344	Bodzioch & Sander, 2012) and in which no LAGs were observed. This suggests that K. perfectus
345	may have reached maturity slightly faster than M. krasiejowensis, but again, additional sampling
346	is required. Variability in ontogenetic trajectories has been previously documented between $D$ .
347	ouazzoui and M. krasiejowensis as a result of differing environmental conditions (Konietzko-
348	Meier & Klein, 2013). As the Chinle depositional basin was positioned closer to the equator in
349	comparison to the environments in which D. ouazzoui and M. krasiejowensis are found (Steiner
350	& Lucas, 2000; Rowe et al., 2007; Zeigler & Geissman, 2011; Nordt, Atchley & Dworkin,
351	2015), it is plausible that the paleoenvironment differed sufficiently from both taxa so as to result
352	in a distinct ontogenetic trajectory in K. perfectus. Additional sampling of material, particularly
353	limb elements, is needed for comparative analyses to assess this possibility.
354	
355	The other unexpected finding of this study was an intercentrum (PEFO 36874a) in the process of
356	undergoing ossification of the notochordal channel (Fig. 4B). This was not evident when
357	examining the external morphology of the specimen, as the notochordal channel or pit is usually
358	filled with secondary minerals. Bone tissue can be clearly seen growing into the channel at the
359	geometric center via deposition of bone on the internal sides of the dorsal and ventral halves
360	(Fig. 4B). The dorsal half appears to be contributing more material through bone deposition, but
361	this requires additional specimens to verify (Fig. 4B). Although this specimen is smaller than the
362	more immature PEFO 4826, this does not contradict our ontogenetic assignment based on
363	examination of the external morphology of other small, elongate intercentra at PEFO. There
364	appears to be some variability in the exact timing of the closure of the notochordal channel, as
365	specimens of similar size and proportion exhibit the full range of conditions, from an open
366	channel to a smooth articular surface lacking any trace of the channel. This could be owing to a
367	number of processes that require additional samples to evaluate, such as the progression of
368	ossification of the vertebral column in the anterior-posterior direction or intraspecific variation in
369	the onset of ossification. If the early stages of vertebral ossification were in some way influenced
370	by environmental factors rather than the size of the animal, developmental plasticity, which
371	occurs in both extant and extinct amphibians, could explain how relatively larger intercentra
372	could sometimes be histologically more immature than smaller ones (Newman, 1992; Schoch,



373	2014). As previously noted, this may also indicate a relatively fast ossification of the notochordal
374	channel.
375	
376	These findings also provide support of niche partitioning between life stages of metoposaurids,
377	which has been suggested in Koskinonodon (Rinehart et al., 2009) and in Metoposaurus (Sulej,
378	2007). Such partitioning could reasonably have created an associated taphonomic bias, which is
379	well documented in both dense bonebeds and more dispersed localities. All known metoposaurid
380	bonebeds have so far produced only large, relatively mature individuals with no evidence of the
381	earliest ontogenetic stages (Case, 1932; Colbert & Imbrie, 1956; Dutuit, 1976; Hunt, 1993; Sulej,
382	2007; Lucas et al., 2010; Brusatte et al., 2015). Furthermore, although fossils from mature
383	individuals of K. perfectus are common in the middle Norian, material referable to juveniles of
384	the taxon is extremely rare, providing another line of support for niche partitioning; to date, only
385	two partial skulls have been described (Zanno et al., 2002; B.M. Gee & W.G. Parker,
386	unpublished data), with a third figured but not described by Hunt (1993). Material of A. gregorii
387	is common in the Redonda Formation in New Mexico but occurs mostly within a single quarry
388	(Gregory's quarry, NMMNH locality 485) (Spielmann and Lucas, 2012). As a result, the relative
389	abundance of A. gregorii may not be the result of ecological turnover as postulated by Hunt
390	(1993) but may represent the preservation of depositional environments inhabited by juveniles of
391	K. perfectus. As bonebeds of mature metoposaurids have been interpreted as evidence of
392	ecological aggregation prior to death, it is not implausible to infer that juveniles may also have
393	naturally aggregated, creating a preservation potential for dense assemblages (Lucas et al., 2010;
394	Brusatte et al., 2015). Based on the isolated and disarticulated nature of most Apachesaurus
395	material, we do not believe these deposits represent mass mortality events, but that they are more
396	likely representative of depositional environments frequented by small metoposaurids over
397	longer durations of time. This hypothesis is supported by a previous study that surveyed blue
398	paleosol localities at PEFO and found that material of many rare taxa, as well as that of $A$ .
399	gregorii, are found mostly within these uncommon horizons (Loughney, Fastovsky & Parker,
400	2011). PFV 040, PFV 215, and potentially PFV 122, the three localities from which specimens
401	for this study were sourced, are all blue paleosol horizons. This lithology is interpreted to have
402	formed in low-energy systems, primarily abandoned channels and ponds adjacent to the main
403	river channel, in contrast to the dominant red floodplain deposits in which fossil material is more





404	fragmentary and isolated (Loughney, Fastovsky & Farker, 2011). The association of
405	Apachesaurus material within these blue paleosol localities supports the hypothesis that deposits
406	that are disproportionately skewed toward fossils of small metoposaurids (exemplified by PFV
407	040 and PFV 215) form in different geologic settings than deposits that are skewed toward large
408	metoposaurids. This in turn supports the hypothesis of natural ecological separation between life
409	stages of metoposaurids. Additionally, taxa that are primarily associated with blue paleosol
410	horizons may not be as stratigraphically restricted as previously thought, and a perceived faunal
411	turnover may in fact be more closely linked to changes in the relative taphonomic conditions of
412	different depositional settings. It is also worth noting that neither A. gregorii nor any other
413	diminutive species of metoposaurid is known outside of North America (Long and Murry, 1995;
414	Spielmann & Lucas, 2012). This is at odds with the conjecture by previous authors that A.
415	gregorii is the most terrestrial of metoposaurids based on the intercentra and rare appendicular
416	material (Hunt, 1993; Sulej, 2007; Spielmann & Lucas, 2012). If this were true, it would be
417	reasonable to expect the taxon or other similarly adapted forms to disperse more widely than
418	aquatic relatives, especially if the pronounced aridification of the Late Triassic led to
419	significantly reduced aquatic environments (Parker & Martz, 2011; Atchley et al., 2013; Nordt,
420	Atchley & Dworkin, 2015), but this pattern is not seen.
421	
422	Conclusions. These findings reiterate the importance of evaluating the potential for
423	morphological variation to be the result of ontogeny, especially when comparing two taxa of
424	vastly different sizes, such as A. gregorii and K. perfectus. Although fossils of A. gregorii are
425	common in late Norian deposits, the vast majority of this material has consisted of elongate
426	intercentra, which we demonstrate here cannot be considered apomorphic. Limited fragmentary
427	pectoral and pelvic material of A. gregorii has been described in the literature, but no
428	justification for ascribing it to the taxon has ever been provided (Hunt, 1993; Long & Murry,
429	1995; Spielmann & Lucas, 2012). Although this material was recovered from the same quarry as
430	cranial and vertebral material, there is no published work suggesting that any of it was found in
431	articulation with any of the diagnostic cranial material (Spielmann & Lucas, 2012). North
432	American metoposaurid specimens are frequently isolated or disarticulated, but this does not
433	negate the importance of reevaluating the taxonomic identity of this material to determine
	negate the importance of recvariating the taxonomic identity of this material to determine
434	whether they preserve robust diagnostic traits. It is possible that these assignments were made





35	solely on the basis of diminutive size (Hunt, 1993; Long & Murry, 1995; Spielmann & Lucas,
36	2012), which cannot be utilized as in species discrimination given the role of ontogeny in
37	producing morphological variation associated with different size bins (Steyer, 2000; Horner and
38	Goodwin, 2009; Witzmann, Scholz & Ruta, 2009). Similarly, although a large number of
39	diagnostic cranial characters have been identified for A. gregorii, only a single character, the
40	shallow otic notch, can be confirmed in any specimens beyond the holotype (Spielmann &
41	Lucas, 2012). The potential for these cranial landmarks to be ontogenetically influenced has not
42	been sufficiently addressed by past workers, in spite of the widespread documentation of
43	morphological changes associated with ontogeny in both extant and extinct amphibians (Hanken,
44	1992; Fröbisch et al., 2010; Schoch, 2014). For example, studies of other Triassic
45	temnospondyls have shown that the otic notch, occipital condyles, and cultriform process (by
46	virtue of its relationship with the interpterygoid vacuities) all play a role in bite force mechanics
47	(Fortuny, Marcé-Nogué & Galobart, 2012; Fortuny et al., 2016; Lautenschlager, Witzmann &
48	Werneburg, 2016). Based on these findings, the presence of shallow otic notches, reduced
49	projection of the occipital condyles, and a wider cultriform process (all supposedly diagnostic
50	traits of A. gregorii) may in fact be influenced by changing biomechanical demands throughout
51	ontogeny, rather than being the result of speciation. The potential for intraspecific variation to
52	exert an influence on metoposaurid morphology has also not been well studied in North
53	American taxa even though studies of bonebeds of M. krasiejowensis and M. algarvensis have
54	demonstrated a higher degree of variability in many cranial regions than previously thought
55	(Sulej, 2007; Brusatte et al., 2015).
56	
57	Finally, we believe that our results provide one line of evidence that A. gregorii is not in fact a
58	distinct species, but rather that it is an early ontogenetic stage of <i>K. perfectus</i> . The stratigraphic
59	distribution that is alleged to reflect ecological turnover is actually controlled by taphonomic bias
60	that results from niche partitioning between different life stages of K. perfectus. The role of
61	ontogeny and intraspecific variation in producing morphological variation in features such as
62	cranial suture patterns, the basicranium, and the otic notch remain relatively unexplored in North
63	American metoposaurids. Discovery and study of additional juvenile specimens is needed to
64	establish a more robust ontogenetic characterization of the earliest stages of metoposaurid
65	development, but our study has also demonstrated that underutilized methods of analysis such as



- paleohistology on existing specimens can shed new light on the paleobiology of extinct taxa withimplications for taxonomy and ontogeny.
- 468
- 469 Acknowledgements. Thanks to Matt Smith (PEFO museum curator) for providing access to
- 470 specimens for histological analysis and to Brad Traver (PEFO Superintendent) for granting
- 471 permission to conduct the destructive analyses. Thanks to Cathy Lash (PEFO fossil preparator)
- 472 for assistance with molding and casting of the specimens and to Yara Haridy (University of
- 473 Toronto) for instruction and guidance on preparation and imaging of thin sections. This is
- 474 Petrified Forest National Park Paleontological Contribution no. 49.

475476

#### References

- Atchley, S.C., Nordt, L.C., Dworkin, S.I., Ramezani, J., Parker, W.G., Ash, S.R., and
- Bowring, S.A. 2013. A linkage among Pangean tectonism, cyclic alluviation, climate
- change and biologic turnover in the Late Triassic: the record from the Chinle Formation,
- southwestern United States. Journal of Sedimentary Research 83(12): 1146-1161. DOI:
- 481 10.2110/jsr.2013.89
- Branson, E.B. and Mehl, M.G. 1929. Triassic amphibians from the Rocky Mountain
- region. University of Missouri Studies 4: 155-239.
- Brusatte, S.L., Butler, R.J., Mateus, O. and Stever, J.S. 2015. A new species of
- 485 *Metoposaurus* from the Late Triassic of Portugal and comments on the systematics and
- biogeography of metoposaurid temnospondyls. Journal of Vertebrate Paleontology 35(3),
- 487 e912988. DOI: 10.1080/02724634.2014.912988
- Case, E.C. 1922. New reptiles and stegocephalians from the Upper Triassic of western
- Texas. Carnegie Institution of Washington 321: 7-84.
- Case, E.C. 1931. Description of a new species of *Buetternia*, with a discussion of the
- brain case. Contributions from the Museum of Paleontology, University of Michigan
- 492 3(11): 187-206.
- Case, E.C. 1932. A collection of stegocephalians from Scurry County, Texas.
- Contributions from the Museum of Paleontology, University of Michigan 4: 1-56.
- Colbert, E.H., and Imbrie, J. 1956. Triassic metoposaurid amphibians. Bulletin of the
- American Museum of Natural History 110(6): 399-452.



497 Danto, M., Witzmann, F. and Fröbisch, N.B. 2016. Vertebral Development in Paleozoic 498 and Mesozoic Tetrapods Revealed by Paleohistological Data. PloS ONE 11(4): 499 e0152586. DOI: 10.1371/journal.pone.0152586 500 Dutuit, J.M. 1976. Introduction à l'étude paléontologique du Trias continental marocain. 501 Description des premiers stegocephales recueillis dans le couloir d'Argana (Atlas 502 occidental). Memoires du Museum National d'Histoire Naturelle, Paris, Series C 36: 1-503 253. 504 • Fortuny, J., Marcé-Nogué, J., Stever, J.S., de Esteban-Trivigno, S., Mujal, E. and Gil, L. 505 2016. Comparative 3D analyses and palaeoecology of giant early amphibians 506 (Temnospondyli: Stereospondyli). Scientific Reports 6: 30387. DOI: 10.1038/srep30387 507 • Fortuny, J., Marcé-Nogué, J., Gil, L. and Galobart, À. 2012. Skull mechanics and the evolutionary patterns of the otic notch closure in capitosaurs (Amphibia: 508 509 Temnospondyli). The Anatomical Record 295(7): 1134-1146. DOI: 10.1002/ar.22486 510 Fröbisch, N.B., Olori, J.C., Schoch, R.R. and Witzmann, F. 2010. Amphibian 511 development in the fossil record. Seminars in Cell & Developmental Biology 21(4): 424-512 431. DOI: 10.1016/j.semcdb.2009.11.001 513 • Hanken, J. 1992. Life history and morphological evolution. Journal of Evolutionary 514 Biology 5(4): 549-557. 515 Heckert, A.B., and Lucas, S.G. 2002. Revised Upper Triassic stratigraphy of the Petrified 516 Forest National Park, Arizona, U.S.A.; pp. 1-36 in A.B. Heckert and S.G. Lucas (eds.), 517 Upper Triassic Stratigraphy and Paleontology. New Mexico Museum of Natural History 518 and Science Bulletin 21. New Mexico Museum of Natural History and Science, 519 Albuquerque. 520 Horner, J.R. and Goodwin, M.B. 2009. Extreme cranial ontogeny in the Upper 521 Cretaceous dinosaur *Pachycephalosaurus*. PLoS ONE 4(10): e7626. DOI: 522 10.1371/journal.pone.0007626 523 Horner, J.R., De Ricglès, A., and Padian, K. 1998. Long bone histology of the 524 hadrosaurid dinosaur Maiasaura peeblesorum: growth dynamics and physiology based 525 on an ontogenentic series of skeletal elements. Journal of Vertebrate Paleontology 20(1): 526 115-129.



- 527 Hunt, A.P. 1993. A revision of the Metoposauridae (Amphibia: Temnospondyli) and 528 description of a new genus from western North America; pp. 67-97 in M. Morales (ed.), 529 Aspects of Mesozoic Geology and Paleontology of the Colorado Plateau. Museum of 530 Northern Arizona Bulletin 59. Museum of Northern Arizona, Flagstaff. 531 • Hunt, A.P., and Lucas, S.G. 1993. Taxonomy and stratigraphic distribution of Late 532 Triassic metoposaurid amphibians from Petrified Forest National Park, Arizona. Journal 533 of the Arizona-Nevada Academy of Science 27(1): 89-96. 534 • Konietzko-Meier, D. and Klein, N. 2013. Unique growth pattern of *Metoposaurus* 535 diagnosticus krasiejowensis (Amphibia, Temnospondyli) from the Upper Triassic of 536 Krasiejów, Poland. Palaeogeography, Palaeoclimatology, Palaeoecology 370: 145-157. 537 DOI: 10.1016/j.palaeo.2012.12.003 538 • Konietzko-Meier, D. and Sander, P.M. 2013. Long bone histology of *Metoposaurus* 539 diagnosticus (Temnospondyli) from the Late Triassic of Krasiejów (Poland) and its 540 paleobiological implications. Journal of Vertebrate Paleontology 33(5):1003-1018. DOI: 541 10.1080/02724634.2013.765886 542 Konietzko-Meier, D., Bodzioch, A. and Sander, P.M. 2012. Histological characteristics 543 of the vertebral intercentra of *Metoposaurus diagnosticus* (Temnospondyli) from the 544 Upper Triassic of Krasiejów (Upper Silesia, Poland), Earth and Environmental Science 545 Transactions of the Royal Society of Edinburgh 103(3-4): 237-250. DOI: 546 10.1017/S1755691013000273 547 • Konietzko-Meier, D., Danto, M. and Gadek, K. 2014. The microstructural variability of the intercentra among temnospondyl amphibians. Biological Journal of the Linnean 548 549 Society 112(4): 747-764. 550 Lautenschlager, S., Witzmann, F. and Werneburg, I. 2016. Palate anatomy and 551 morphofunctional aspects of interpterygoid vacuities in temnospondyl cranial 552 evolution. The Science of Nature 103(9-10): 79. DOI: 10.1007/s00114-016-1402-z 553 • Long, R.A. and Murry, P.A. 1995. Late Triassic (Carnian and Norian) Tetrapods from the 554
- Southwestern United States. New Mexico Museum of Natural History and Science 555 Bulletin 4. New Mexico Museum of Natural History and Science, Albuquerque.
- 556 Loughney, K.M., Fastovsky, D.E. and Parker, W.G. 2011. Vertebrate fossil preservation 557 in blue paleosols from the Petrified Forest National Park, Arizona, with implications for



558 vertebrate biostratigraphy in the Chinle Formation. Palaios, 26(11): 700-719. DOI: 559 10.2110/palo.2011.p11-017r 560 • Lucas, S.G., Rinehart, L.F., Krainer, K., Spielmann, J.A. and Heckert, A.B. 2010. 561 Taphonomy of the Lamy amphibian quarry: a Late Triassic bonebed in New Mexico, 562 USA. Palaeogeography, Palaeoclimatology, Palaeoecology 298(3): 388-398. DOI: 563 10.1016/j.palaeo.2010.10.025 564 • Mueller, B.D. 2007. Koskinonodon Branson and Mehl, 1929, a replacement name for the 565 preoccupied temnospondyl Buettneria Case, 1922. Journal of Vertebrate Paleontology 566 27(1): 225-225. DOI: 10.1671/0272-4634(2007)27[225:KBAMAR]2.0.CO;2 • Mukherjee, D., Ray, S. and Sengupta, D.P. 2010. Preliminary observations on the bone 567 568 microstructure, growth patterns, and life habits of some Triassic temnospondyls from 569 India. Journal of Vertebrate Paleontology 30(1): 78-93. DOI: 570 10.1080/02724630903409121 571 • Newman, R.A. 1992. Adaptive plasticity in amphibian metamorphosis. BioScience 42(9): 572 671-678. 573 • Nordt, L., Atchley, S. and Dworkin, S. 2015. Collapse of the Late Triassic megamonsoon 574 in western equatorial Pangea, present-day American Southwest. Geological Society of 575 America Bulletin 127(11-12): 1798-1815. DOI: 10.1130/B31186.1 576 Padian, K. 2013. Why study the bone microstructure of fossil tetrapods?, pp. 1-12 in K. Padian and E.-T. Lamm (eds.), Bone Histology of Fossil Tetrapods. University of 577 578 California Press, Berkeley. 579 • Parker, W.G. and Martz, J.W. 2010. The Late Triassic (Norian) Adamanian–Revueltian 580 tetrapod faunal transition in the Chinle Formation of Petrified Forest National Park, 581 Arizona. Earth and Environmental Science Transactions of the Royal Society of 582 Edinburgh 101(3-4): 231-260. DOI: 10.1017/S1755691011020020 Rinehart, L.F. and Lucas, S.G. 2009. Limb allometry and lateral line groove development 583 584 indicates terrestrial-to-aquatic lifestyle transition in Metoposauridae (Amphibia: 585 Temnospondlyi) [paper no. 96-14]. Geological Society of America Abstracts with 586 Program 41(7): 263.



587 Rowe, C.M., Loope, D.B., Oglesby, R.J., Van der Voo, R. and Broadwater, C.E. 2007. 588 Inconsistencies between Pangean reconstructions and basic climate 589 controls. Science 318(5854): 1284-1286. DOI: 10.1126/science.1146639 590 Sanchez, S. and Schoch, R.R. 2013. Bone histology reveals a high environmental and 591 metabolic plasticity as a successful evolutionary strategy in a long-lived homeostatic 592 Triassic temnospondyl. Evolutionary Biology 40(4): 627-647. DOI 10.1007/s11692-013-593 9238-3 594 Schoch, R.R. 2014. Life cycles, plasticity and palaeoecology in temnospondyl 595 amphibians. Palaeontology, 57(3): 517-529. DOI: 10.1111/pala.12100 596 Spielmann, J.A. and Lucas, S.G. 2012. Tetrapod Fauna of the Upper Triassic Redona 597 Formation East-central New Mexico: The Characteristic Assemblage of the Apachean 598 Land-vertebrate Faunachron. New Mexico Museum of Natural History and Science 599 Bulletin 55. New Mexico Museum of Natural History and Science, Albuquerque. Steiner, M.B. and Lucas, S.G. 2000. Paleomagnetism of the Late Triassic Petrified Forest 600 601 Formation, Chinle Group, western United States: Further evidence of "large" rotation of 602 the Colorado Plateau. Journal of Geophysical Research 105(B11): 25-791. 603 Stever, J.S. 2000. Ontogeny and phylogeny in temnospondyls: a new method of analysis. Zoological Journal of the Linnean Society 130(3): 449-467. 604 605 DOI: 10.1111/j.1096-3642.2000.tb01637.x Stever, J.S., Laurin, M., Castanet, J. and De Ricglès, A. 2004. First histological and 606 607 skeletochronological data on temnospondyl growth: palaeoecological and 608 palaeoclimatological implications. Palaeogeography, Palaeoclimatology, 609 Palaeoecology 206(3): 193-201. DOI: 10.1016/j.palaeo.2004.01.003 610 Sulei, T. 2007. Osteology, variability, and evolution of *Metoposaurus*, a temnospondyl 611 from the Late Triassic of Poland. Palaeontologia Polonica 64: 29-139. 612 Warren, A. and Snell, N. 1991. The postcranial skeleton of Mesozoic temnospondyl 613 amphibians: a review. Alcheringa 15(1): 43-64. 614 Werning, S. 2012. The ontogenetic osteohistology of *Tenontosaurus tilletti*. PLoS ONE 615 7(3): e33539. DOI: 10.1371/journal.pone.0033539



616 • Witzmann, F., Scholz, H. and Ruta, M. 2009. Morphospace occupation of temnospondyl 617 growth series: a geometric morphometric approach. Alcheringa, 33(3): 237-255. DOI: 618 10.1080/03115510903043606 619 • Witzmann, F. and Soler-Gijón, R. 2010. The bone histology of osteoderms in 620 temnospondyl amphibians and in the chroniosuchian *Bystrowiella*. Acta Zoologica 91(1): 96-114. DOI: 10.1111/j.1096-3642.2009.00599.x 621 622 • Zanno, L. E., Heckert, A. B., Krzyzanowski, S. E., and Lucas, S. G. 2002. Diminutive 623 metoposaurid skulls from the Upper Triassic Blue Hills (Adamanian: latest Carnian) of Arizona; pp. 121-126 in A.B. Heckert and S.G. Lucas (eds.), Upper Triassic Stratigraphy 624 625 and Paleontology. New Mexico Museum of Natural History and Science Bulletin 21. 626 New Mexico Museum of Natural History and Science, Albuquerque. 627 Zeigler, K.E. and Geissman, J.W. 2011. Magnetostratigraphy of the Upper Triassic Chinle Group of New Mexico: Implications for regional and global correlations among 628 629 Upper Triassic sequences. Geosphere 7(3): 802-829. DOI: 10.1130/GES00628.1 630 631 **Figure Captions** 632 Figure 1. Map of PEFO showing localities of sampled specimens. Localities and associated specimens are as follows: PFV 122 (Blue Mesa Member): PEFO 4826 and PEFO 38726; PFV 633 040 (Petrified Forest Member): PEFO 38645; PFV 215 (Petrified Forest Member): PEFO 36874, 634 635 PEFO 16696, and PEFO 35392. 636 Figure 2. Stratigraphic column of PEFO showing position of sampled specimens and 637 **localities.** Localities and associated specimens are as follows: PFV 122 (Blue Mesa Member): 638 PEFO 4826 and PEFO 38726; PFV 040 (Petrified Forest Member): PEFO 38645; PFV 215 (Petrified Forest Member): PEFO 36874, PEFO 16696, and PEFO 35392. 639 Figure 3. Photographs of sampled specimens in anterior and lateral profiles. (A) PEFO 640 641 38726, (B) PEFO 4826, (C) PEFO 38645, (D-E) PEFO PEFO 36874, (F-G) PEFO 35392, (H-J) 642 PEFO 16696. Order of photographed specimens mirrors their listed order in Table 1. 643 Figure 4. Microphotographs of the sagittal sections of sampled specimens. (A) PEFO 36874a, (B) PEFO 16696a, (C) PEFO 4826, (D) PEFO 16696b, (E) PEFO 38645, (F) PEFO 644 645 36874b (G) PEFO 35392a, (H) PEFO 16696c, (I) PEFO 35392, (J) PEFO 38726. Scale bars 646 equal to 4 mm.

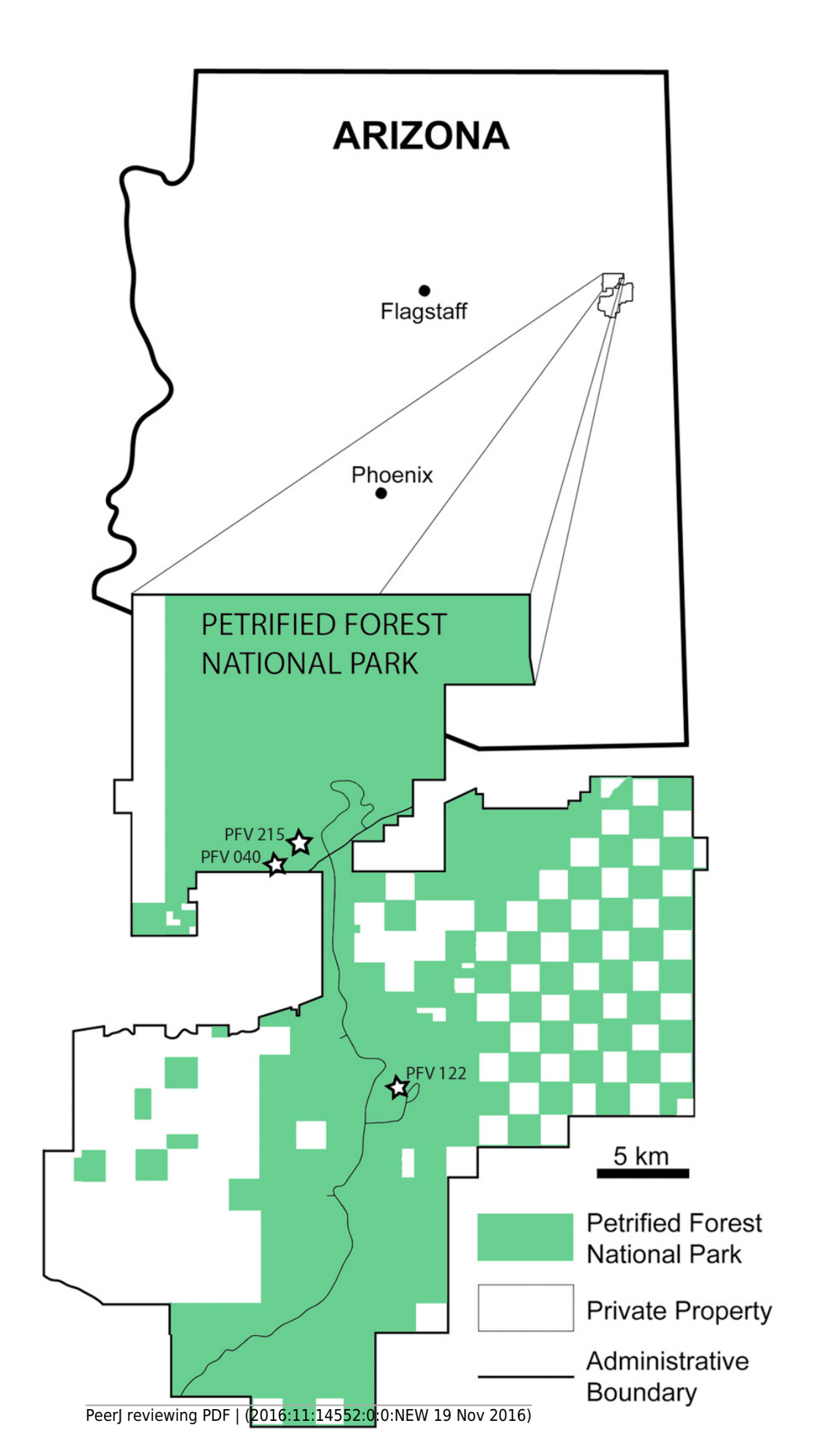


- 647 Figure 5. Microphotographs of the notochordal channel in three small specimens. (A) PEFO
- 648 4826 (B) PEFO 36874a, (C) PEFO 16696a. Scale bars equal to 1 mm.
- 649 Figure 6. Microphotographs of the periosteal region in three small specimens. (A) PEFO
- 4826 (B) PEFO 36874a, (C) PEFO 16696a, (D) PEFO 16696b. Scale bars equal to 1 mm.
- Figure 7. Microphotographs of the dorsal endochondral region in three small specimens.
- 652 (A) PEFO 4826 (B) PEFO 36874a, (C) PEFO 16696a. Scale bars equal to 1 mm.
- 653 Figure 8. Microphotograph of the external cortex in large intercentra. (A) PEFO 38645, (B)
- PEFO 35392a, (C) PEFO 16696c, (D) PEFO 38726. Arrows indicate the position of the LAGs in
- 655 PEFO 38726. Scale bars equal to 1 mm.



Map of PEFO showing localities of sampled specimens.

Localities and associated specimens are as follows: PFV 122 (Blue Mesa Member): PEFO 4826 and PEFO 38726; PFV 040 (Petrified Forest Member): PEFO 38645; PFV 215 (Petrified Forest Member): PEFO 36874, PEFO 16696, and PEFO 35392.

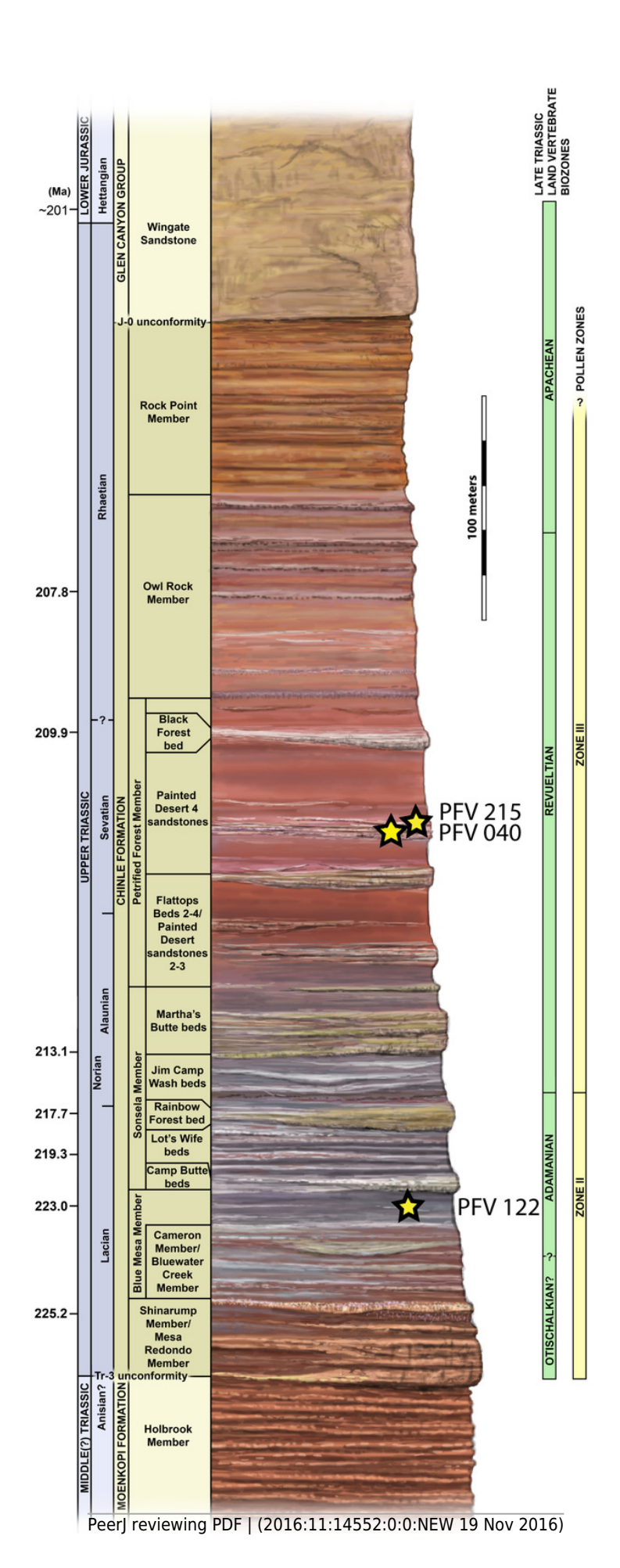




Stratigraphic column of PEFO showing position of sampled specimens and localities.

Localities and associated specimens are as follows: PFV 122 (Blue Mesa Member): PEFO 4826 and PEFO 38726; PFV 040 (Petrified Forest Member): PEFO 38645; PFV 215 (Petrified Forest Member): PEFO 36874, PEFO 16696, and PEFO 35392.



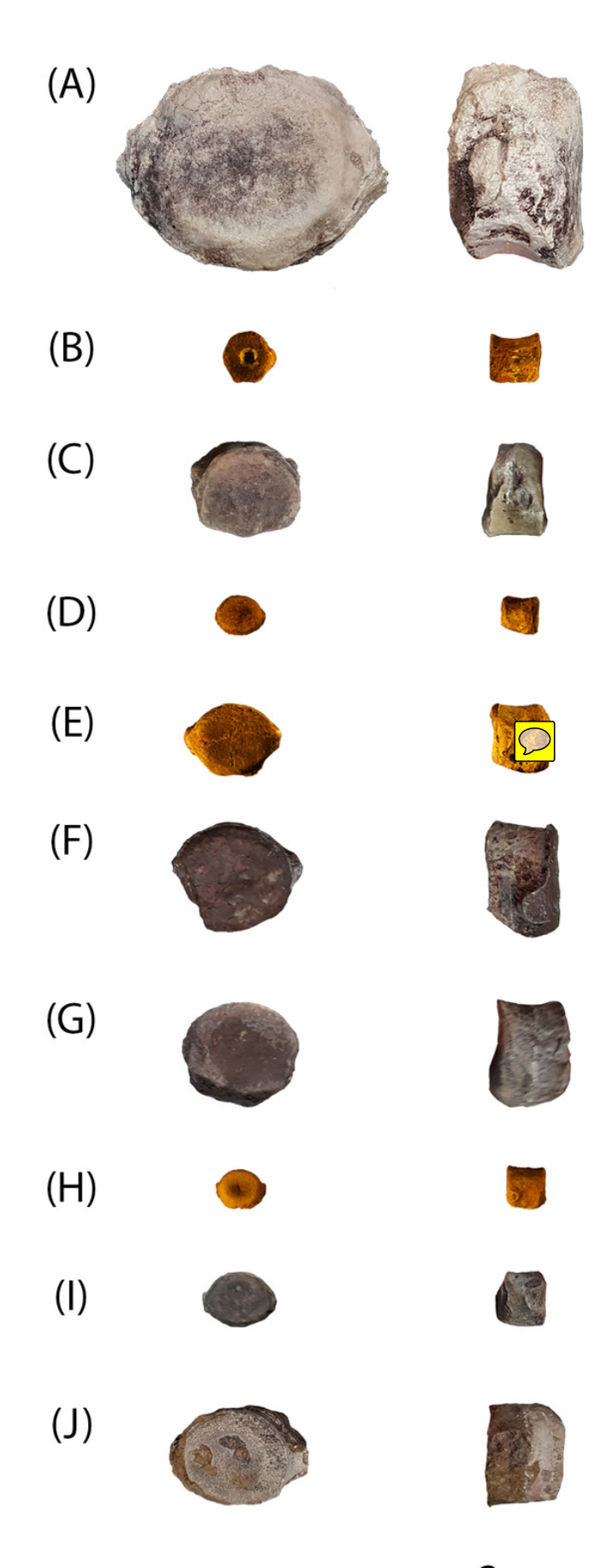




Photographs of sampled specimens in anterior and lateral profiles.

(A) PEFO 38726, (B) PEFO 4826, (C) PEFO 38645, (D-E) PEFO PEFO 36874, (F-G) PEFO 35392,

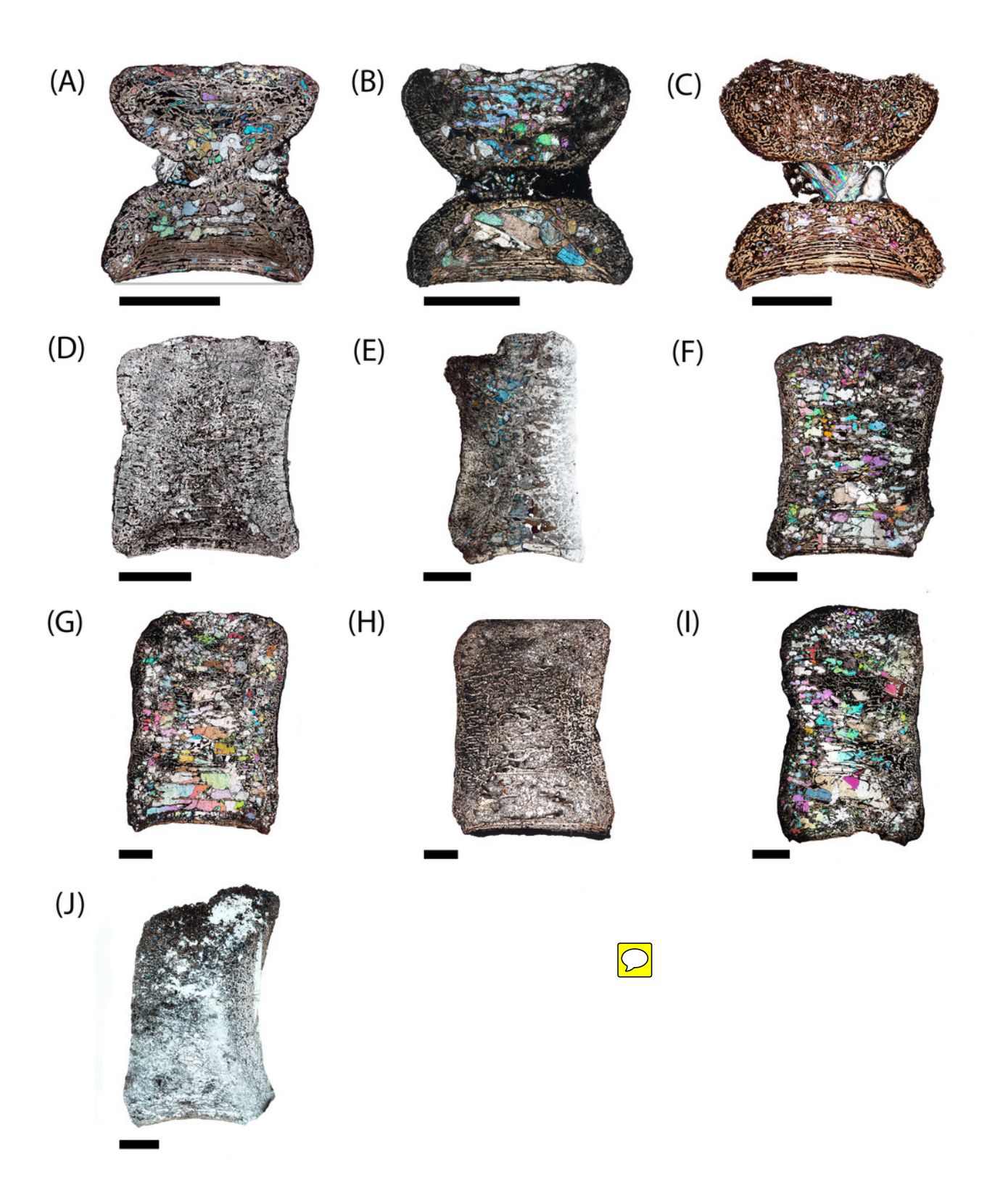
(H-J) PEFO 16696. Order of photographed specimens mirrors their listed order in Table 1.





Microphotographs of the sagittal sections of sampled specimens.

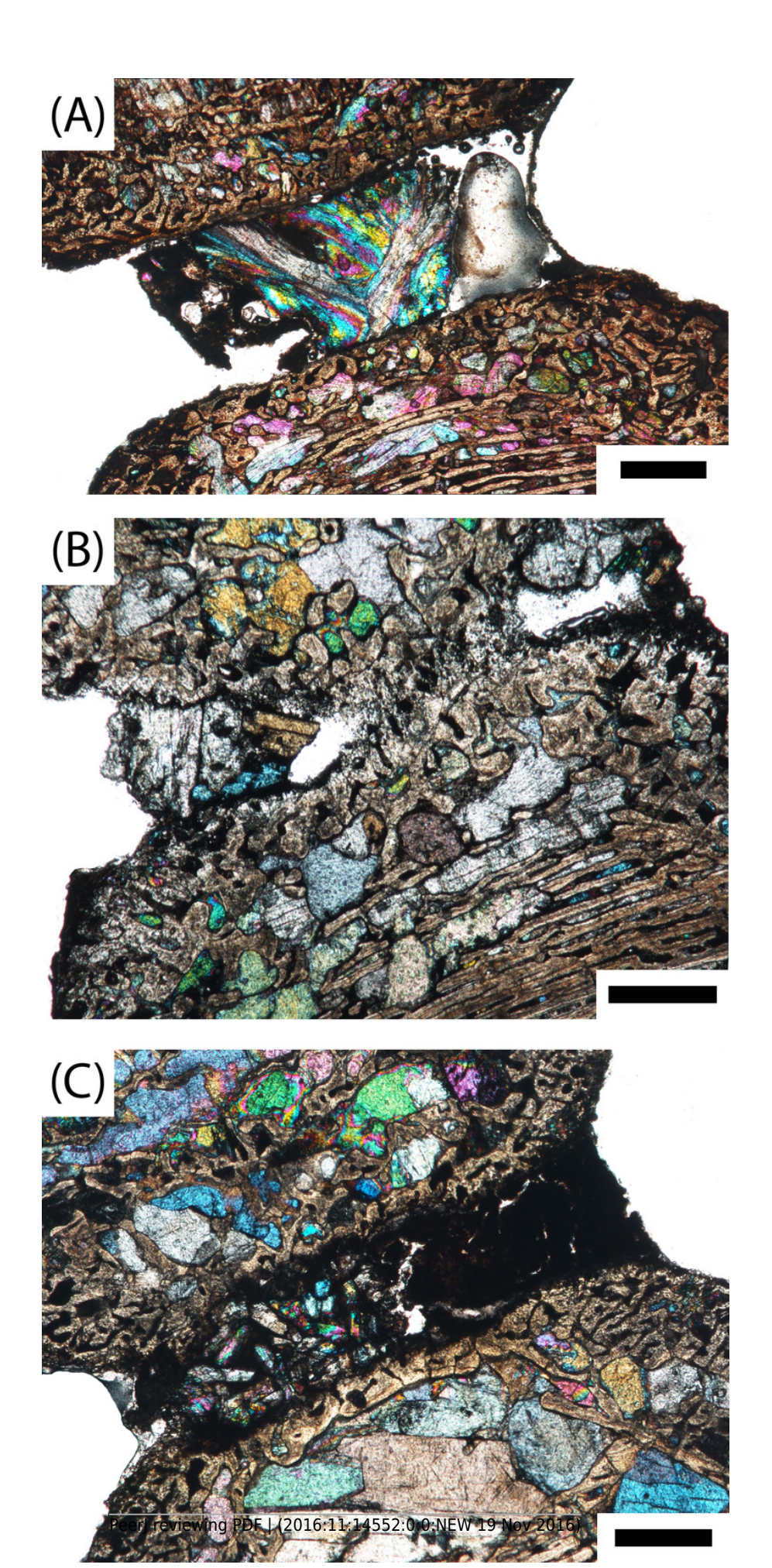
(A) PEFO 36874a, (B) PEFO 16696a, (C) PEFO 4826, (D) PEFO 16696b, (E) PEFO 38645, (F) PEFO 36874b (G) PEFO 35392a, (H) PEFO 16696c, (I) PEFO 35392, (J) PEFO 38726. Scale bars equal to 4 mm.





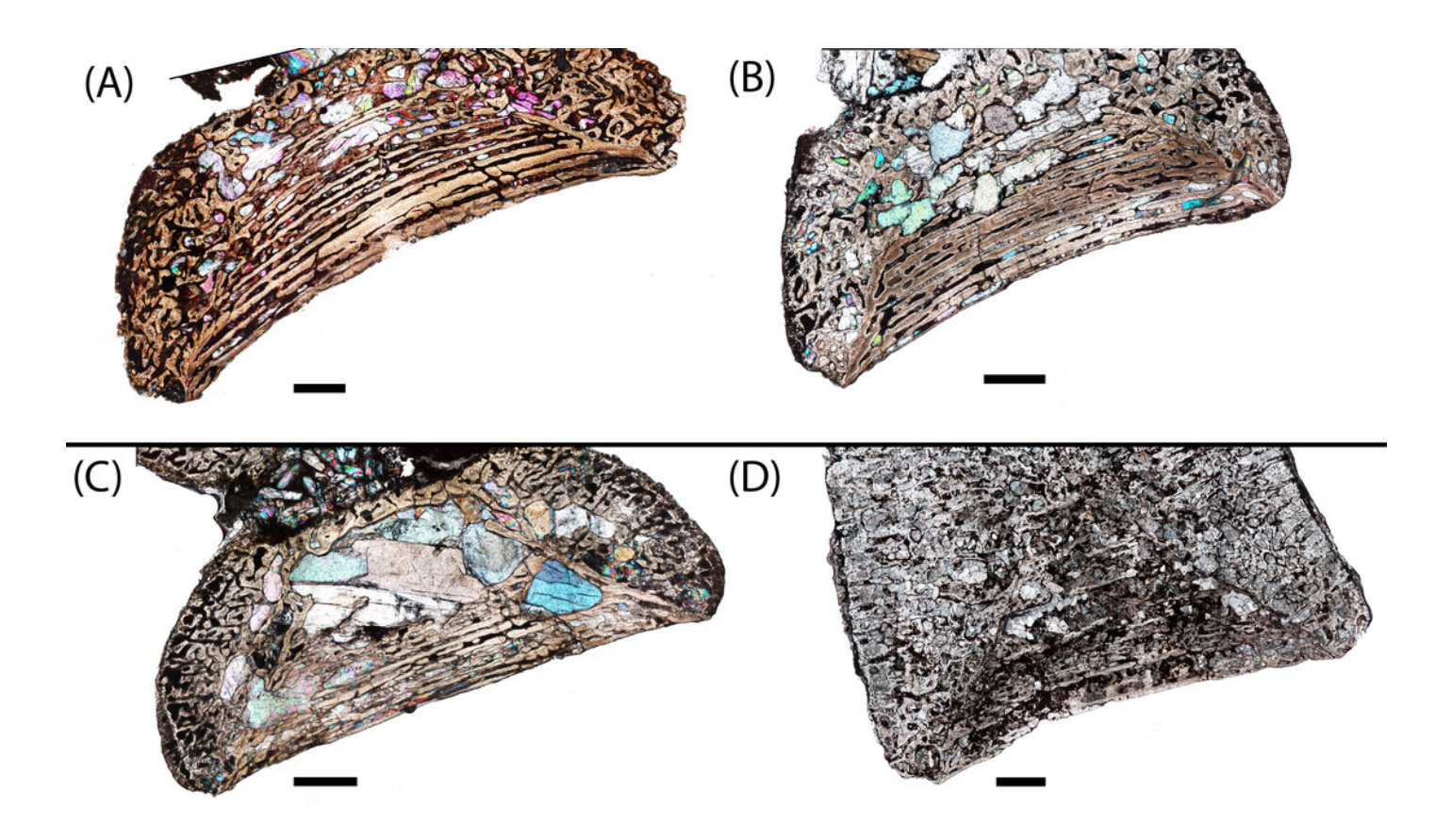
Microphotographs of the notochordal channel in three small specimens.

(A) PEFO 4826 (B) PEFO 36874a, (C) PEFO 16696a. Scale bars equal to 1 mm.



Microphotographs of the periosteal region in three small specimens.

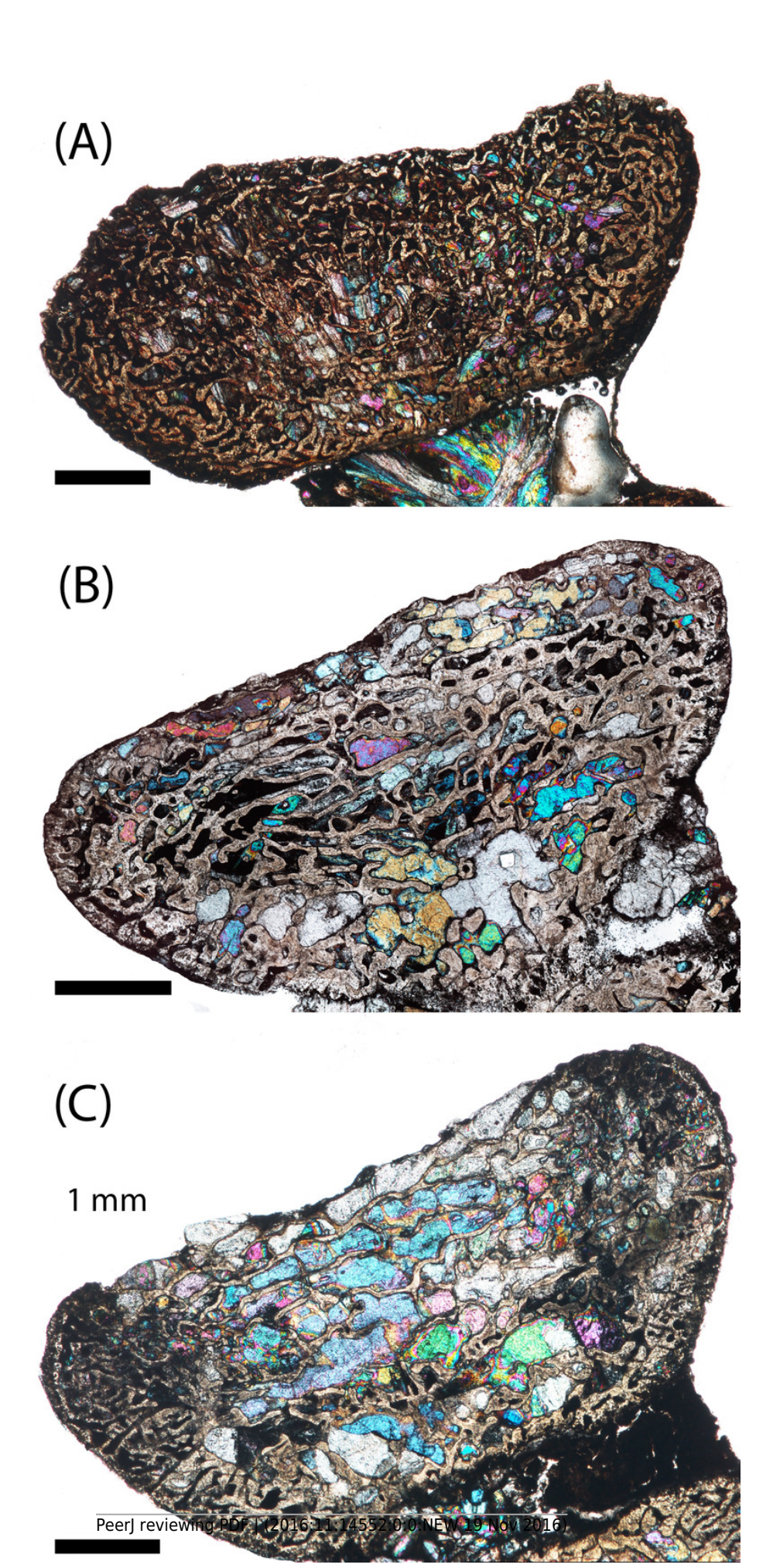
(A) PEFO 4826 (B) PEFO 36874a, (C) PEFO 16696a, (D) PEFO 16696b. Scale bars equal to 1 mm.





Microphotographs of the dorsal endochondral region in three small specimens.

(A) PEFO 4826 (B) PEFO 36874a, (C) PEFO 16696a. Scale bars equal to 1 mm.



Microphotograph of the external cortex in large intercentra.

(A) PEFO 38645, (B) PEFO 35392a, (C) PEFO 16696c, (D) PEFO 38726. Arrows indicate the position of the LAGs in PEFO 38726. Scale bars equal to 1 mm.

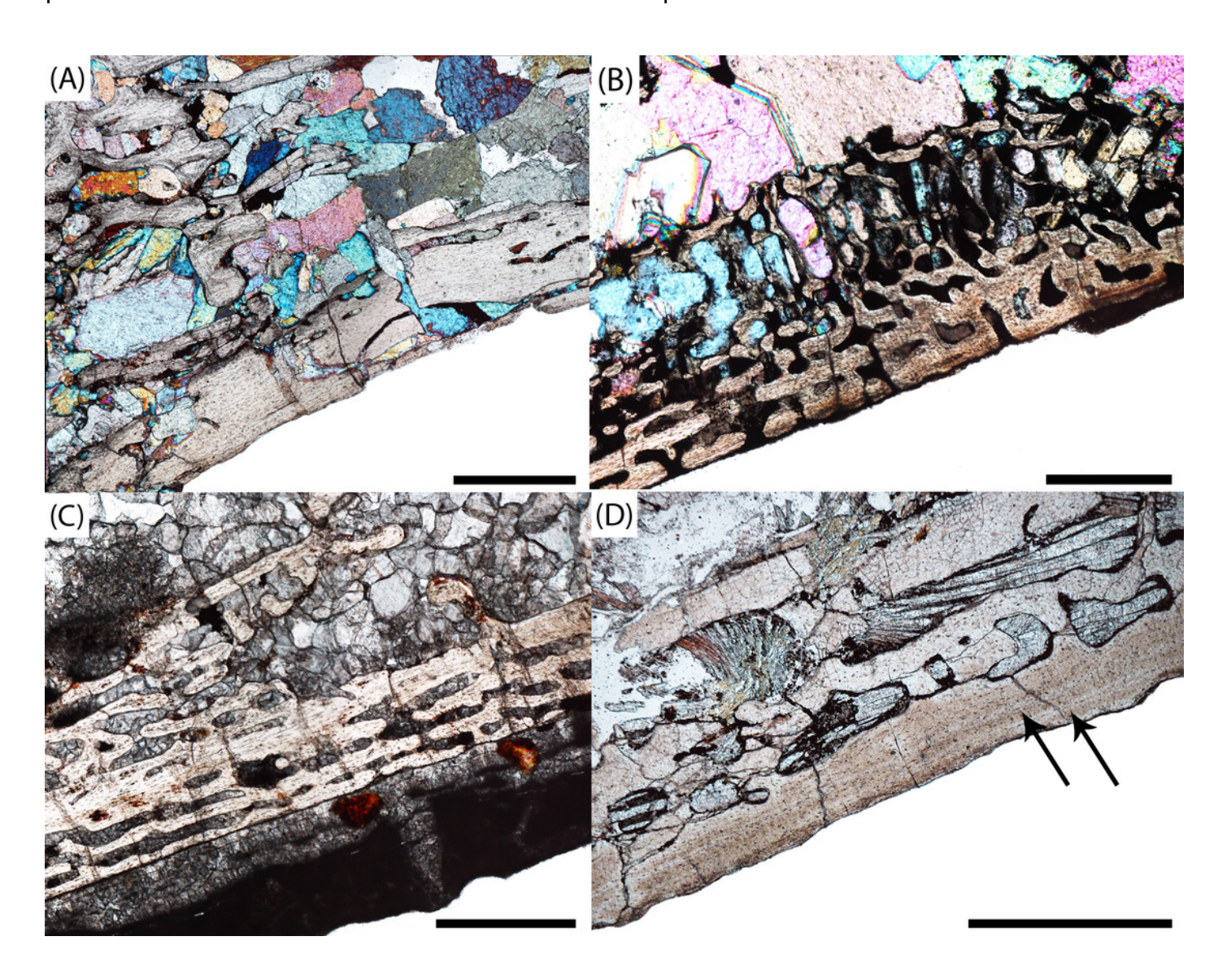




#### Table 1(on next page)

Summary of intercentra analyzed in this experiment.

For specimens with multiple elements, the listed order reflects their order by size, from smallest to largest. Letter assignments for multi-element specimens were created for the purpose of this publication to facilitate their references throughout the text. Measurements were performed in the same manner as in Konietzko-Meier, Bodzioch, & Sander (2012), where length is in the anteroposterior axis, width is in the mediolateral axis, and height is in the dorsoventral axis. *Geologic member abbreviations: BMM – Blue Mesa Member; PFM – Petrified Forest Member.* 

Table 1. Summary of intercentra analyzed in this experiment. For specimens with multiple elements, the listed order reflects their order by size, from smallest to largest. Letter assignments for multi-element specimens were created for the purpose of this publication to facilitate their references throughout the text. Measurements were performed in the same manner as in Konietzko-Meier, Bodzioch, & Sander (2012), where length is in the anteroposterior axis, width is in the mediolateral axis, and height is in the dorsoventral axis. *Geologic member abbreviations: BMM – Blue Mesa Member; PFM – Petrified Forest Member.* 

Specimen	Estimated	Cutting	Length	Width	Height	W:L	Geologic
number	position	plane	(mm)	(mm	(mm)		member
PEFO 38726	anterior dorsal	sagittal	22.98	55.32	46.91	2.40	BMM
PEFO 4826	dorsal	sagittal	10.25	10.55	12.71	1.03	BMM
PEFO 38645	presacral	sagittal	10.99	21.90	19.32	1.99	PFM
PEFO 36874a	dorsal	sagittal	7.65	10.72	8.85	1.40	PFM
PEFO 36874b	perisacral	sagittal	11.85	19.63	17.25	1.65	PFM
PEFO 35392	mid-dorsal	sagittal	15.43	28.27	25.74	1.83	PFM
PEFO 35392b	anterior dorsal	sagittal	15.37	25.89	24.72	1.68	PFM
PEFO 16696a	pre-sacral	sagittal	8.22	10.22	9.09	1.24	PFM
PEFO 16696b	mid-dorsal	sagittal	9.52	15.96	12.11	1.67	PFM
PEFO 16696c	mid-dorsal	sagittal	16.60	26.83	16.13	1.61	PFM



#### Table 2(on next page)

Summary of major histological landmarks identified in the sampled specimens.

For specimens with multiple elements, the listed order reflects their order by size, from smallest to largest. Dots indicate the presence of the structure in specimens.



- 1 Table 2. Summary of major histological landmarks identified in the sampled specimens. For
- 2 specimens with multiple elements, the listed order reflects their order by size, from smallest to largest.
- 3 Dots indicate the presence of the structure in specimens.

Specimen ID	Periosteal bone	External cortex	LAGs	HOS
PEFO 38726	•	•	•	4
PEFO 4826	•			2
PEFO 38645	•	•		3
PEFO 36874a	•			2
PEFO 36874b	•	•		3
PEFO 35392	•	•		3
PEFO 35392b	•	•		3
PEFO 16696a	•			2
PEFO 16696b	•			2
PEFO 16696c	•	•		3

4